Diffusion and segregation of Sr in glassy carbon: Model and analysis

Johan B. Malherbe* and O.S.Odutemowo

Department of Physics, University of Pretoria, Pretoria, 0028, South Africa

* Corresponding author. Email: johan.malherbe@up.ac.za

Highlights

- An equation was derived from the Fick diffusion equation for an implanted profile with a segregating force term added.
- The equation fitted well to implanted Sr profiles annealed at different temperatures.
- The segregation force field results in a general velocity of the impurity atoms.
- There are no such velocity measurements reported in order to compare our values.
- The velocities found are of the correct order of magnitude and increase with annealing temperature.

Abstract

Some diffusing systems segregation towards the surface also occurs. Such a system can be described by adding a force-induced velocity term to the Fick diffusion equation. The profile of an implanted material is usually Gaussian or at least very near a Gaussian function. In this paper this Fick partial differential equation in a force field was solved for an initially Gaussian profile. The simulated profiles exhibit the expected behavior. 200 keV implanted strontium into glassy carbon and isochronically annealed in vacuum from 300 °C to 900 °C for 1 h. The Sr profiles were determined by RBS (Rutherford backscattering spectrometry). They showed both diffusion and segregation between 400 °C to 900 °C. These profiles were fitted to the abovementioned solution to extract the diffusion coefficient and segregation drift velocity at each annealing temperature. In the temperature range 400 °C to 800 °C the diffusion coefficient had an activation energy for diffusion of 0.20 eV and 1.2 nm^2/s for the pre-exponential factor D_0. The segregation velocity, which is directly proportional to the segregating force, increased with increasing temperature. At annealing temperature of 400 °C the average drift velocity towards the surface was 39 pm/s and at 900 °C it was an order of maginitude higher at 0.34 nm/s.

Graphical abstract

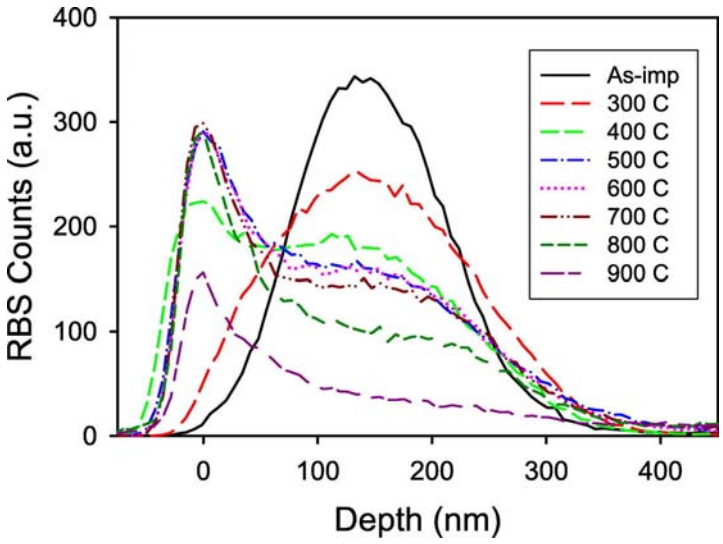

Keywords: Segregation; Fick diffusion equation, Gaussian profile

1. INTRODUCTION

Diffusion and surface segregation are two phenomena in materials science which have the same fundamental driving force, i.e. minimization of the Gibbs free energy of the total system. In diffusion the motion of the atoms is usually described by a random walk process. In a uniform material the diffusion profile of a highly diluted impurity is given by the Fick diffusion equations [1,2]. Because diffusion is linked to the motion of atoms, it usually increases with increasing temperature. In a limited temperature range, the diffusion coefficient usually has an Arrhenius dependency on temperature. In surface segregation (also grain boundary segregation) a diluted impurity diffuses to the surface to often form a monolayer on the surface. There are many different models to describe the experimental results [3-5]. The temperature dependence of segregation is complex with a general increase with increasing temperature. However, there are also cases where the segregated impurity on the surface starts to dissolve back into the bulk above a certain temperature in agreement with the Langmuir-MacLean theory [6-8]. Surprisingly, there are no reported studies of a quantitative analysis of both segregation and diffusion in a system.

There are many cases where species implanted in a solid exhibit both diffusion and segregation above certain temperatures. This is especially true for glassy carbon

implanted with Ce [9], Cd [10], In [11], Xe [12], N, [13], Eu [14], co-implanted Sr and Ag [14] and for Sr [15-19]. It also occurs in other systems such as iodine in 6H-SiC co-implanted with I and Ag [20].

Most diffusion studies are performed during isochronal annealing conditions. Although structural changes and the diffusion and segregation of strontium implanted in glassy carbon has been reported previously [15], [16], [17], [18], [19], [21], the isochronal diffusion of Sr has not been reported in depth. Consequently, in this study we quantitatively report on its diffusion and segregation.

For this purpose a formula is needed which can be fitted to the experimental depth profiles of the implanted and annealed Sr. As was mentioned above, there is no publication giving such a formula. Consequently, a model is developed in this paper to describe Fickian diffusion where segregation also occurs. The time-dependent Fick diffusion equation is solved for a force field which forces an impurity to move preferentially towards the surface in addition to Fickian diffusion.

2. MODEL: SIMULTANEOUS FICKIAN DIFFUSION AND SEGREGATION

2.1 Derivation

This derivation below relies heavily on the treatment by Boltaks [2]. If a force acts on diffusing particles it gives the particles an average velocity v. This force-induced flow causes the normal diffusional flow (flux) J_D (the rate at which the diffusing particles passes through a unit cross-sectional area) given by Fick's first law

$$J_D = -D\frac{\partial N}{\partial x} \tag{1}$$

to be modified by adding another term flow term $J_v = Nv$. N is the concentration of the impurity in the substrate. Thus the diffusion flow then becomes

$$J = -D\frac{\partial N}{\partial x} + Nv \tag{2}$$

Using (2), Fick's second law becomes

$$\frac{\partial N}{\partial t} = D\frac{\partial^2 N}{\partial x^2} - v\frac{\partial N}{\partial x} \tag{3}$$

D is the diffusion coefficient and t is the diffusing time. The substitution by Smoluchowski [22]

$$N(x,t,v) = \exp\left(\frac{v}{2D}x - \frac{v^2}{4D}t\right)N^*(x,t) \tag{4}$$

simplifies (3) to

$$\frac{\partial N^*}{\partial t} = D\frac{\partial^2 N^*}{\partial x^2} \tag{5}$$

(5) is similar to the normal Fick diffusion equation. Consequently, the same methods to solve it can be used to eventually solve (3). The general solution for an isotropic, semi-infinite body, i.e. a body bounded at $x = 0$ and extending to - ∞, is given by [2]

$$N^*(x,t,v) = \frac{1}{2\sqrt{\pi D t}}\int_0^\infty \left[N^*(\xi,0,v)\exp\left(-\frac{(\xi - x)^2}{4Dt}\right) + N_1^*(-\xi,0,v)\exp\left(-\frac{(\xi + x)^2}{4Dt}\right)\right]d\xi \tag{6}$$

Where $N_1^*(-\xi,0,v)$ must be determined from the boundary conditions. Take

$$N_1^*(-\xi,0,v) = -kN^*(\xi,0,v) \tag{7}$$

(7) is reasonable because if one solves (3) for a perfect sink at the surface, i.e. $x = 0$, then $k = +1$; while for a perfect reflecting boundary at $x = 0$, $k = -1$. So for a general case where there where there is either a sink or a reflection or a combination of the two at the surface that $-1 \le k \le 1$. The same condition was used to solve the normal Fickian diffusion equation for an initial Gaussian profile [23]. From (4)

$$N(\xi,0,v) = \exp\left(\frac{v\xi}{2D}\right) N^*(\xi,0,v)$$

Thus

$$N^*(\xi,0,v) = N(\xi,0,v)\exp\left(-\frac{v\xi}{2D}\right) \tag{7}$$

Similarly

$$N_1^*(-\xi,0,v) = N_1(-\xi,0,v)\exp\left(\frac{v\xi}{2D}\right) \tag{8}$$

Substitute (7) and (9) in (6) and using again the Smoluchowski transformation (4), (6) eventually becomes

$$N(x,t,v) = \frac{1}{2\sqrt{\pi Dt}}\int_0^\infty N(\xi,0,v)\left[\exp\left(-\frac{\{\xi-(x-vt)\}^2}{4Dt}\right) - k\exp\left(-\frac{v\xi}{D}\right)\exp\left(-\frac{\{\xi+(x-vt)\}^2}{4Dt}\right)\right]d\xi \tag{9}$$

For an isotropic medium implanted with mono-energetic impurity atoms, the initial profile can be assumed to be Gaussian with projected range R_p and range straggling ΔR_p, i.e.

$$N(\xi,0) = A_0\exp\left(-\frac{(\xi-R_p)^2}{2\Delta R_p^2}\right) \tag{10}$$

Substituting (10) with known values for A_0, R_p and ΔR_p, into (9) and doing all the integrals and algebra, the solution is giving by

$$N(x,t,v) = \frac{A_0\Delta R_p}{2\sqrt{\left(2Dt+\Delta R_p^2\right)}}\cdot\exp\left\{-\frac{\{R_p-(x-vt)\}^2}{2\left(2Dt+\Delta R_p^2\right)}\right\}\cdot$$

$$< 1 + \operatorname{erf}\left(\frac{\left\{2DtR_p + \Delta R_p^2 (x - vt)\right\}}{\sqrt{4\Delta R_p^2 Dt \cdot \left(2Dt + \Delta R_p^2\right)}} \right) > - \; k \exp\left[\frac{\Delta R_p^2 vtx - 2DtR_p x}{Dt \cdot (2Dt + \Delta R_p^2)} \right] \cdot$$

$$< 1 - \operatorname{erf}\left(\frac{\left\{-2DtR_p + 2vt\Delta R_p^2 + \Delta R_p^2 (x - vt)\right\}}{\sqrt{4Dt \cdot \Delta R_p^2 \left(2Dt + \Delta R_p^2\right)}} \right) > \qquad (11)$$

2.2 Simulated profiles

In this subsection simulated diffusion and segregation profiles are considered for the two limiting cases, k = 1 and k = - 1. For all the model simulations typical implantation parameter values were used for the initial Gaussian profile, viz. R_p = 120 nm, ΔR_p = 25 nm, A_0 = 0.5 atomic percent, and also a realistic diffusion coefficient D = 1 x 10^{-19} m^2 s^{-1} = 0.1 nm^2 s^{-1} with diffusion times of 1 h, 3 h, and 5 h. Two values were chosen for the force velocity, viz. a surface segregation velocity of v = - 0.005 nm/s (i.e. a segregating force towards the surface) and a force which drives the impurity deeper into the bulk with v = + 0.005 nm/s. The implantation parameters were chosen to depict a deep implanted profile where the surface concentration of the implanted material is effectively zero. Furthermore, the concentration of the implanted impurity is low to comply with Fickian diffusion conditions.

In Figure 1 a simulated diffusion and segregation profile, for the case k = -1, is given at different times t. The most obvious observation is that for $v > 0$ the profile moves preferentially towards the bulk. For $v < 0$ the reverse happens, exhibiting a kind of surface segregation. The position of the maximum of the peak shifts from R_p to approximately $R_p + vt$. At longer diffusion times for $v < 0$ the profiles becomes too distorted to distinguish the peak. This happens because no diffusant is lost through the surface and the atoms are reflected back towards the bulk. Due to the diffusion process being fundamentally a random walk process, there is conglomeration at the surface. At the lowest diffusion time the diffused profile is still fairly Gaussian with a lowering of the maximum peak height due to this broadening of the peak.

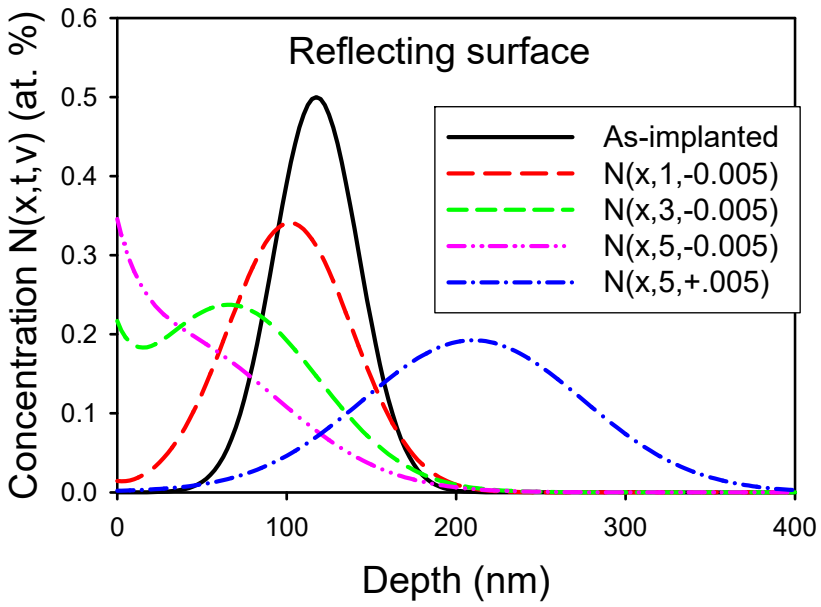

Figure 1. Simulated diffusion and segregation profiles, i. e. equation (11), for the case $k = -1$ (i.e. a perfectly reflecting boundary at $x = 0$), is given for different diffusion times t (in hours) and force velocities v (in nm/s) indicated in the figure. Typical implantation values were used for initial Gaussian profile: R_p = 120 nm, ΔR_p = 25 nm, A_0 = 0.5 atomic percent, and a diffusion coefficient $D = 0.1$ nm^2 s^{-1}.

In Figure 2 the same parameters used in Figure 1 are used in a simulated diffusion profile, for the case $k = 1$. This case represents a perfect sink for the impurity at the surface. In practical terms it illustrates the diffusion of an impurity with a high vapour pressure leading to a complete sublimation of the impurity atoms into the environment when they reach the surface of the substrate. This is a more common occurrence than the previous example considered in Figure 1. Similar observations as seen in Figure 1, can be made here for the lower diffusion times, i.e. a symmetric broadening of the peak and lowering of the peak height. Again, unless the profile becomes too distorted due to the loss of diffusant through the surface, the position of the maximum of the peak shifts from R_p to approximately $R_p + vt$. For values near $x = 0$, the boundary condition of a sink, forces the diffused profile to become 0 and the diffused profiles deviate from being approximately Gaussian, especially for larger diffusion times, i.e. larger Dt values.

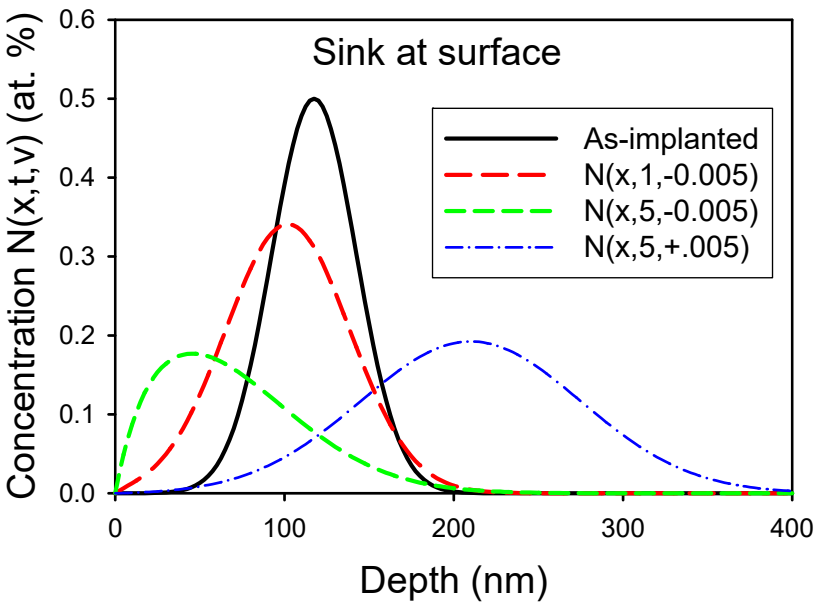

Figure 2. A simulated diffusion and segregation profile, i. e. equation (11), for the case $k = 1$ (i.e. a perfect sink at the surface), is given for different diffusion times t (in hours) and force velocities v (in nm/s) indicated in the figure. Typical implantation values were used for initial Gaussian profile: R_p = 120 nm, ΔR_p = 25 nm, A_0 = 0.5 atomic percent, and a diffusion coefficient $D = 0.1$ nm^2 s^{-1}.

In many systems, there is neither a perfect sink nor perfect reflection at the surface. Such cases are represented by $-1 < k < 1$. Such conditions appear in the diffusion and segregation profiles for Sr in glassy carbon shown later in this paper.

2.3 Discussion of the model

That both diffused profiles for the two limiting cases for the parameter k in (11) remain largely Gaussian in shape at the lower diffusion times, is due to the fact that the error function erf $z \approx 1$ for $z >> 1$ and erf $z = 0$ for $z = 0$. Thus, the pre-(square) bracket term in (11), i.e.

$$\frac{A_0 \cdot \Delta R_p}{2\sqrt{2Dt + \Delta R_p{}^2}} e^{\left(\frac{\{R_p - (x - vt)\}^2}{4Dt + 2\Delta R_p^2}\right)} \qquad (12)$$

is the dominating term in (11) except for small x and large t values. From this it is clear why the peak position shifts approximately from R_p to $R_p + vt$. The Gaussian function (12), which is broader than the original implanted distribution, due to factor $2\Delta R_p^2 = 4Dt$ in the quotient of the argument in the exponential function. Consequently, it is convenient to fit the experimental values first to such a Gaussian function to obtain an approximate solution for the diffusion coefficient D and for force parameter v, which then together with the estimates for the surface factor k, result in an efficient fitting of the full equation (11).

The energetic bombarding ions can cause several effects in the substrate material which can influence the diffusion kinetics and mechanisms. The most obvious of these effects is radiation damage which can lead to radiation enhanced and/or radiation induced diffusion [24]. The above solution(s) can handle these cases as long as there are still Fickian diffusion and Gibbsian segregation . Radiation damage can also result in the trapping of the implanted species by defect complexes [25]. These diffusion traps are temperature dependent, usually causing no or little diffusion below the trap releasing temperature, and then normal diffusion and segregation above that temperature. The above solution can be applied to such systems above at these higher temperatures. Another phenomenon which also acts as a kind of diffusion trap is the chemical compound formation between the implanted atoms and substrate atoms. Sputtering of and substrate topography development on the substrate, due to the ion bombardment, do not affect the diffusion and segregation mechanisms but can lead to erroneous depth profiles [26,28].

3. Experimental

SIGRADUR® G glassy carbon samples from Hochtemperatur Werkstoffe (HTW), Germany were used for this research. The samples were mechanically polished on an ATM Saphir 500 polisher with 1µmµm and 0.25 µm diamond solutions respectively before being cleaned using an alkaline soap solution in an ultrasonic bath. This was followed sequentially by de-ionized water (several times) and methanol. The de-ionized water was used to remove the soap solution from the sample. The samples were dried by blowing nitrogen gas on them for a few minutes and then placed in an

oven at 50 °C for 1 h so as to remove volatile impurities on the surface of the carbon samples.

200 keV strontium ions were implanted at room temperature to a fluence of 2×10^{16} cm^{-2}. The flux was kept at about 10^{12} ions/cm^2 in order to avoid annealing effects. During implantation the substrate reached a maximum temperature of about 55 °C. After implantation, the samples were cut into suitable sizes followed again by the above cleaning procedure. The samples were annealed in a quartz vacuum tube furnace which anneals up to 1000 °C. Sequential isochronal annealing for 1 h was done from 300 °C in steps of 100 °C up to 900 °C. A turbo pump provided a vacuum with a base pressure of about 10^{-7} mbar. A thermocouple was placed close to the sample in order to measure and monitor its temperature.

The strontium implanted glassy carbon samples were analysed using Rutherford backscattering spectroscopy before and after every annealing. The samples were irradiated with alpha particles of energies 1.4 MeV and 1.6 MeV. A total charge of 8 μC was used throughout this study during a reading. In order to ensure accuracy and noise reductions, repeated readings were taken and averaged. An analysing current of 15 nA was used in order to prevent pile up of the backscattered helium particles. The scattering angle was 165^o. The fitting details of the strontium profiles to the Eq. (11) were discussed above.

4. Experimental results and discussion

All the RBS Sr profiles are shown in Fig. 3. The statistical error in the RBS counts was estimated from the average variation in the counts in the depth region 400 to 450 nm. Using the maximum of the as-implanted profile, this error was 3.5%. The as-implanted Sr data fitted well to a Gaussian profile – see Fig. 4. As can be seen, the sample annealed at 300 °C broadened fairly symmetrical. This is an indication that only diffusion took place with no segregation. Consequently, this profile was fitted to the solution of the (normal) Fick diffusion equation for an initial Gaussian impurity profile given in Malherbe et al. [25] – also depicted in Fig. 4. Again an excellent fit was obtained.

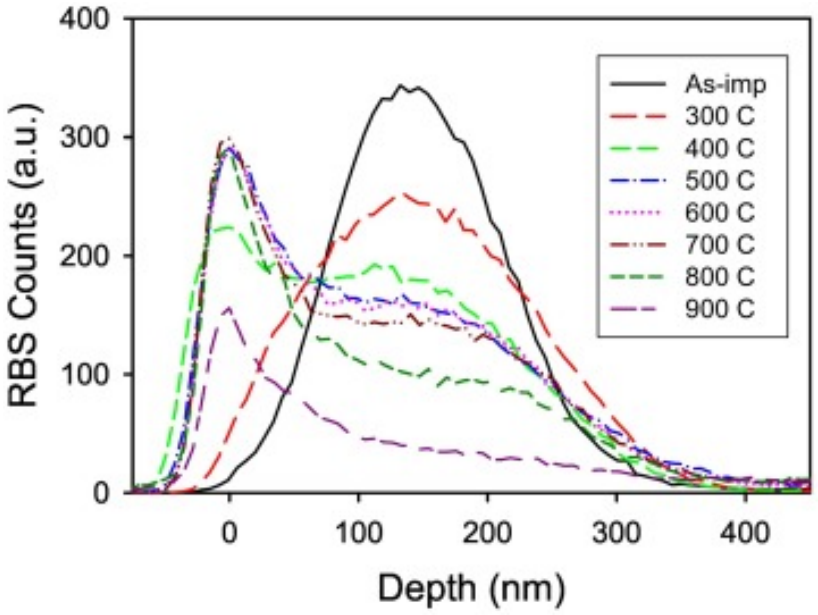

Fig. 3. RBS spectra of 200 keV strontium implanted in glassy carbon and sequentially vacuum annealed for 1 h at the temperatures indicated in the legend.

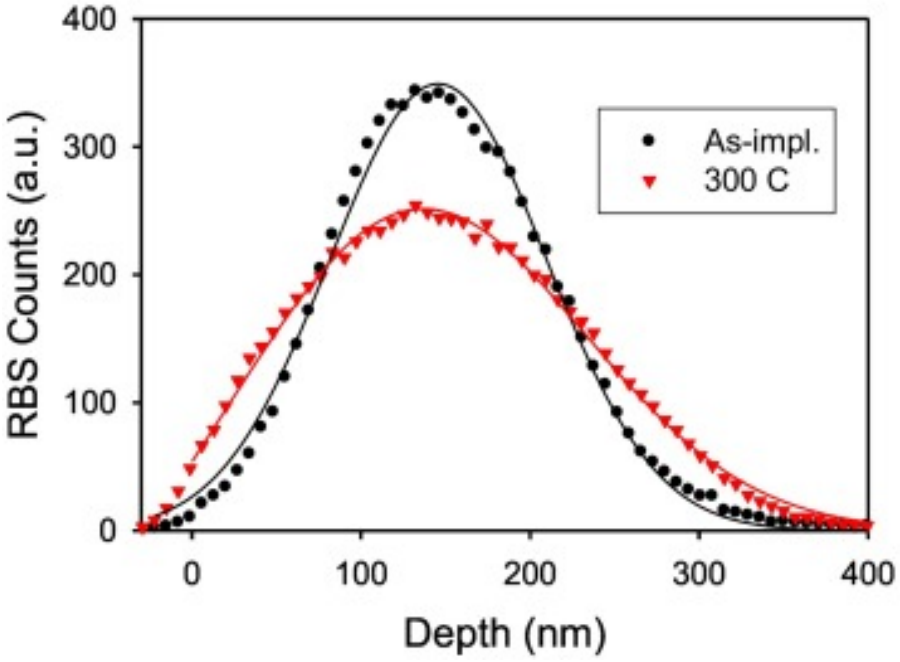

Fig. 4. The Sr RBS data points for the as-implanted sample (dots) and the one annealed at 300 °C for 1 h (triangles). The solid lines are a Gaussian fit to the as-implanted data and the solution to the Fick equation for diffusion for an initially Gaussian impurity profile [25].

From Fig. 3 it can be seen that with annealing at 400 °C and sequential annealing at higher temperatures, the Sr profiles became asymmetric towards to surface indicating segregation towards the surface. A surface peak also developed. The original peak of the implanted sample as well as for the 300 °C annealed sample was still visible as a local maxima but at the two highest annealing temperatures the Sr profile has segregated too much to the surface with a dramatic decline in the areas under the Sr curves. This indicates that strontium sublimated into the vacuum at the higher annealing temperatures as shown in Fig. 5, which gives the retained ratio of strontium in the glassy carbon samples after each annealing temperature. The ratio was taken to be equal to the normalised area under each Sr profile. The area under the as-implanted Sr profile is given at 25 °C and was also taken as the standard for normalisation. When taking the 3.5% statistical error into account it is clear that no strontium was lost up to an annealing temperature of 700 °C, where only a small amount was lost. The loss increased dramatically at the two highest temperatures with only about 36% being retained after annealing at 900 °C. This not surprising as the melting point of strontium is 777 °C with an equilibrium vapour pressure of about 100 Pa at 717 °C which rises exponentially to 1 k Pa at 866 °C.

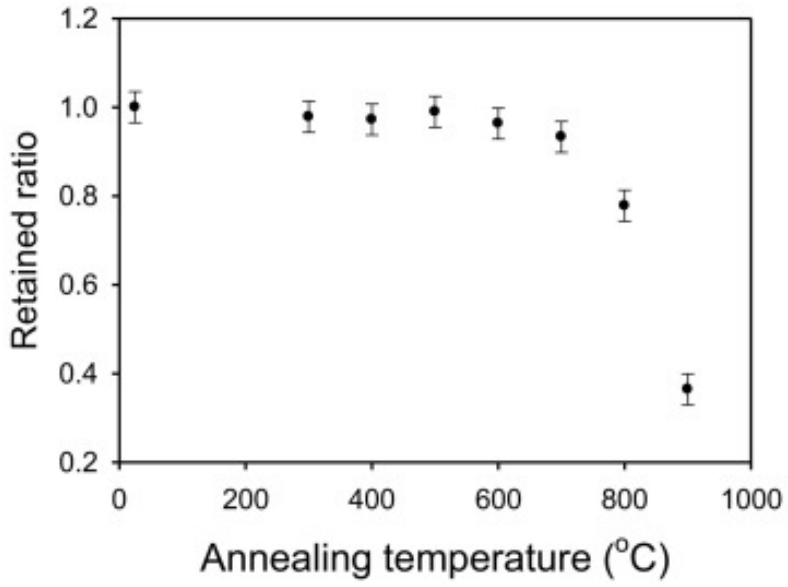

Fig. 5. Retained ratio of strontium in the glassy carbon samples after each annealing temperature. The value of the as-implanted sample is given at 25 °C. The error bars represent the 3.5% statistical error.

The Sr profiles which exhibited a collective movement towards the surface were fitted to Eq. (11). Examples of the fitting are shown in Fig. 6 for the two extreme annealing temperatures. From the fittings the diffusion parameter D and the segregation velocity v were extracted for each temperature. An Arrhenius plot of the diffusion coefficients is shown in Fig. 7. There is a good ($r^2 = 0.974$) linear regression to the data of 400 °C to 800 °C giving an activation energy for diffusion of 0.20 eV and 1.2 nm^2/s for the pre-exponential factor D_0. This low activation energy confirms that there many open (interstitial and vacancy) sites in an amorphous material allowing impurity atoms to easily diffuse in the glassy carbon. In glasses the activation energy is related with size of the diffusing atom with smaller sizes having lower activation energies since less they require less strain energy to dilate the cavities in the amorphous matrix [29]. The strontium atom is relatively large compared to many other metallic atoms.

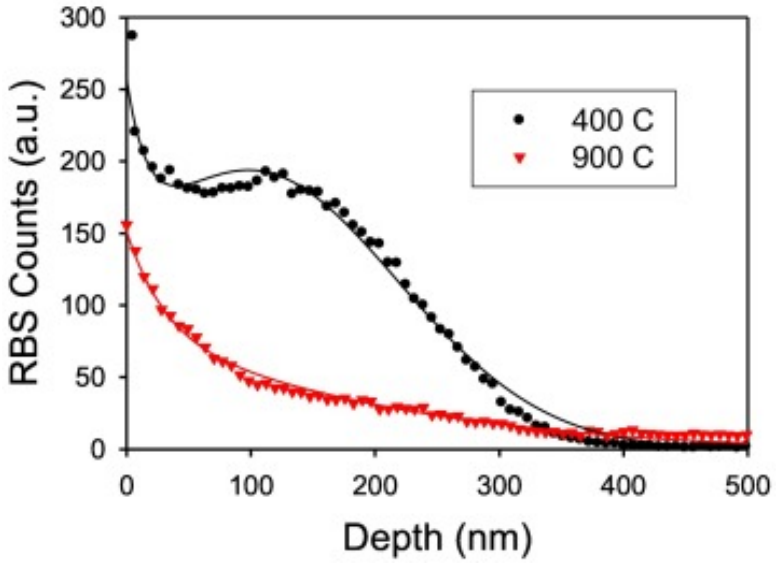

Fig. 6. The fitting of Eq. (11) to the Sr profiles of samples at the annealing temperatures of 400 °C and 900 °C.

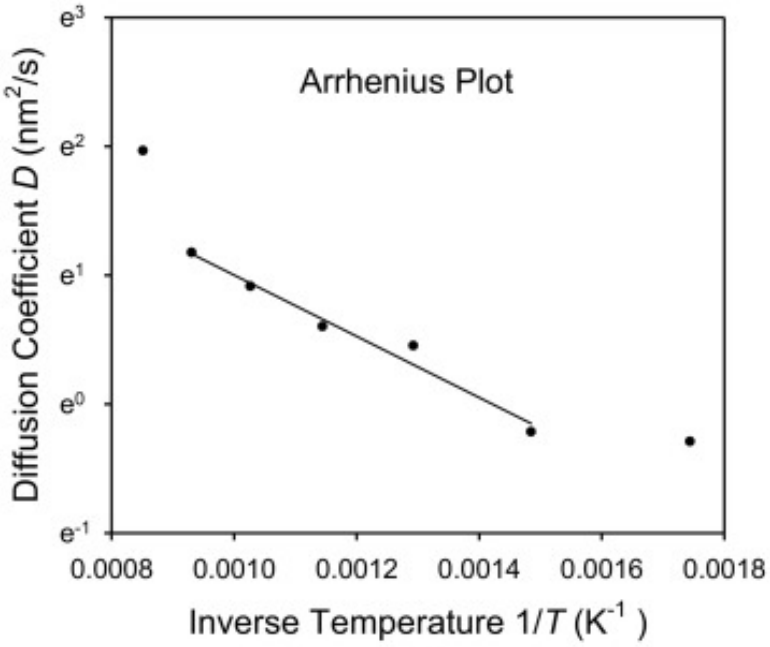

Fig. 7. An Arrhenius plot of the diffusion coefficients. Also shown is the linear regression line to selected data.

In Fig. 7, the diffusion coefficient values of the samples annealed at the two end temperatures deviate significantly from the regression line. There are two possible reasons for each temperature. The one reason for the deviation of the diffusion coefficient at 900 °C can be seen in Fig. 6. At that temperature most of the Sr atoms (only about 36% of the original number remained) have segregated to the surface and were sublimated into the vacuum. Thus, too few atoms remained to give a reliable multi-parameter fitting. The other reason might be a different diffusion mechanism starts operated at this temperature giving rise to another activation energy. To test this, annealing at other (including higher) temperatures are needed. The loss of Sr atoms from the glassy carbon substrate will complicate such measurements.

The Sr depth profiles after annealing at 300 °C for 1 h exhibited only pure Fickain diffusion and no segregation while at the higher temperatures (400 °C and higher) both diffusion and segregation occurred. This also affected the activation energies. Malherbe et al. [19] also determined diffusion coefficients of Sr implanted into glassy carbon when linearly heating the samples and simultaneously taking RBS depth profiles. The strontium only started to diffuse at 414 °C. From this temperature up to

454 °C the diffusion had one activation energy while from 458 °C to 558 °C it had another activation energy. Above 558 °C the segregation started to dominate. The reason why the temperature dependence is so different from the present resulsts is based on the time span for the diffusion to occur. The present resulsts were obtained after isochronal heating for 1 h at a particular temperature while in the other study the temperature was continuously increased with effectively a very small time in between the temperatures. The extent of diffusion is a product of both the diffusion coefficient and time therefore a direct comparison between the two studies cannot be made. The essential point is that at lower temperature the activation activation energy is different to that at the higher temperatures.

The absolute value of the velocity v increased with increasing temperature. This not surprising because both diffusion and segregation are thermally activated processes. According the Nernst-Einstein theory (see [29]) the virtual force acting on the particles to give them an average drift velocity is given by the negative gradient of the potential field ϕ (usually the chemical potential μ for normal diffusion). The velocity v is equal to

$$v = Force \times Mobility = -\frac{1}{N_A}\frac{d\varphi}{dx}M$$

where N_A is Avogadro's number and M is the mobility, i.e. the drift velocity when a unit force is acting. Thus, the flux due to this force is given by

$$J_v = Nv = N\frac{1}{N_A}\frac{d\varphi}{dx}M$$

To make the terms unit-less, the theory to develop the above further is usually done by dividing by k_BT where k_B is the Boltzmann constant. Consequently, we depict velocity (we used speed) as a function of 1/T in Fig. 8. A regression line is drawn for the data of the four lowest temperatures. It resulted in an extremely good fit ($r^2 = 0.993$) considering the fact that these speeds were obtained from a multi-parameter fit. The two speeds after annealing at 800 °C and 900 °C do not agree with the linear trend of the lower temperatures. This is either due to too many Sr atoms

escaping from the substrate thereby affecting the fitting procedure, or that another kind of segregation mechanism occurred at these two higher temperatures.

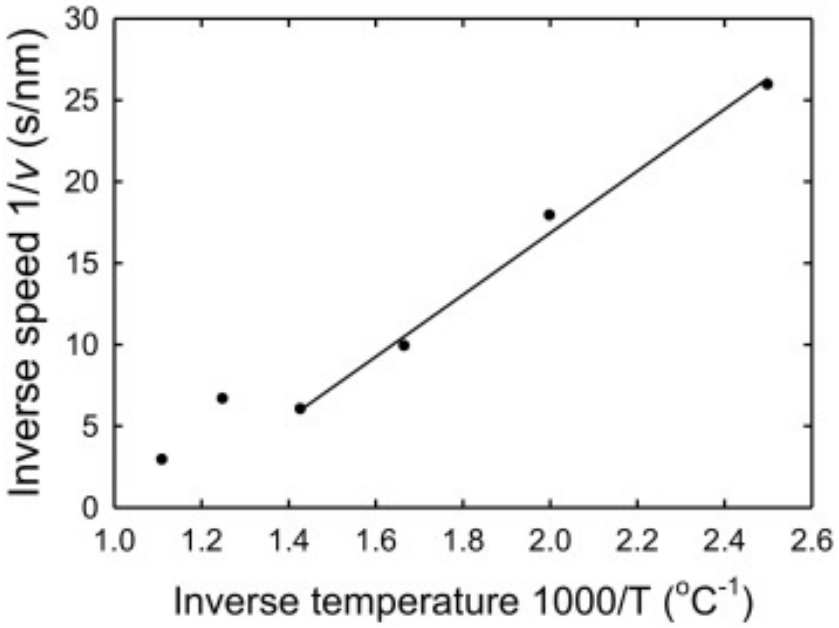

Fig. 8. The temperature dependence of values obtained for the segregation speeds.

5. SUMMARY

Implanted strontium in glassy carbon shows that at some annealing temperatures there is diffusion and segregation towards the surface taking place. Such a system can be described by adding a force-induced velocity term to the Fick diffusion equation. The profile of an implanted material is usually Gaussian or at least very near a Gaussian function. In this paper this Fick partial differential equation in a force field was solved for an initially Gaussian profile. Diffused and segregated profiles were simulated for the two extreme cases, a perfect sink and a perfect reflective boundary at the surface. The simulated profiles exhibit the behavior expected for these two cases.

The solution obtained were used to fit the profiles of implanted Sr into glassy carbon and isochronically annealed from 400 °C to 900 °C in a vacuum to extract the diffusion coefficient and segregation drift velocity at each annealing temperature. In the temperature range 400 °C to 800 °C the diffusion coefficient had an activation energy for diffusion of 0.20 eV and 1.2 nm^2/s for the pre-exponential factor D_0. The

segregation velocity, which is directly proportional to the segregating force, increased with increasing temperature. At annealing temperature of 400 °C the average drift velocity towards the surface was 39 pm/s and at 900 °C it was an order of maginitude higher at 0.34 nm/s.

Funding

We have not received any funding for this project.

6. REFERENCES

1. H. Mehrer, *Diffusion in solids*, Springer, Berlin, 2007.
2 B.I. Boltaks, *Diffusion in Semiconductors*, Infosearch Ltd, New York, 1963.
3. G.A. Somorjai,. *Introduction to surface chemistry and catalysis*. Chap. 3, 1st ed., Wiley, Chichester, 1994.
4. J. du Plessis, G.N van Wyk, Model for surface segregation in multicomponent materials Part 1I Comment on other segregation analyses, J. Phys. Chem. Solids 49 (1989) 1441-1458.
5. P. Lejček, L. Zhei, S. Hofmann, M. Šob, Applied Thermodynamics: Grain Boundary Segregation, Entropy 16 (2014) 1462-1483.
6. J.K.O. Asante, J.J. Terblans, W.D. Roos, Segregation of Sn and Sb in a ternary Cu(1 0 0)SnSb alloy, Appl. Surf. Sci. 252 (2005) 1674-1678.
7. J.J. Terblans, H.C. Swart, The Segregation of Bi and S from a Cu(Bi,S) Ternary System, e-J Surf Sci Nanotech 7 (2009) 480-485.
8. X.L. Yan, J.Y. Wang, H.C. Swart, J.J. Terblans AES study of Cu and S surface segregation in a ternary Ni-Cu(S) alloy in combination with a linear heating method, J Alloys Comp 768 (2018) 875 - 882.

9. D.F.Langa, N.G. Van der Berg, E. Friedland, J.B. Malherbe, A.J. Botha, P. Chakraborty, E. Wendler, W. Wesch, Heat treatment of glassy carbon implanted with cesium at room and high temperatures, Nucl. Instrum. Methods Phys. Res. B 273 (2012) 68-71.

10. T.T. Hlatshwayo, L.D. Sebitla, E.G. Njoroge, M. Mlambo, J.B. Malherbe, Annealing effects on the migration of ion-implanted cadmium in glassy carbon, Nucl. Instrum. Methods Phys. Res. B 395 (2017) 34-38.

11. E.G. Njoroge, L.D. Sebitla, C.C. Theron, M. Mlambo, T.T. Hlatshwayo, O.S. Odutemowo, V.A. Skuratov, E. Wendler, J.B. Malherbe, Structural modification of indium implanted glassy carbon by thermal annealing and SHI irradiation, Vacuum 144 (2017) 63-71.

12. M.Y.A. Ismail, J.B. Malherbe, O.S. Odutemowo, E.G. Njoroge, T.T. Hlatshwayo, M. Mlambo, E. Wendler, Investigating the effect of heat treatment on the diffusion behaviour of xenon implanted in glassy carbon, Vacuum 149 (2018) 74-78.

13. H. Kröger, C. Ronning, H. Hofsäss, P. Neumaier, A. Bergmaier, L. Go¨rgensb, G. Dollinger, Diffusion in diamond-like carbon, Diamond Rel. Mater. 12 (2003) 2042-2050.

14. M.F. Kenari, T.T. Hlatshwayo, O.S. Odutemowo, T.M. Mohlala, E. Wendler, J.B. Malherbe, Migration behavior of 100° C europium ion implantation in glassy carbon, in: 2018 22nd Int. Conf. Ion Implant. Technol., IEEE, 2018: pp. 377–380.

15. O.S. Odutemowo, M.S. Dhlamini, E. Wendler, D.F. Langa, M.Y.A. Ismail, J.B. Malherbe, Effect of heat treatment on the migration behaviour of Sr and Ag co-implanted in glassy carbon, Vacuum 171 (2020) 109027 (7 pages).

16. O.S. Odutemowo, J.B. Malherbe, C.C. Theron, E.G. Njoroge, E Wendler, "*In-situ* RBS studies of strontium implanted glassy carbon", Vacuum 126 (2016) 101-105.

17. O.S. Odutemowo, J.B. Malherbe, L.C. Prinsloo, E.G. Njoroge, R. Erasmus, E. Wendler, A. Undisz, M. Rettenmayr, Structural and surface changes in glassy carbon due to strontium implantation and heat treatment, J. Nucl. Mater. 498 (2018) 103-116.

18. J.B. Malherbe, O.S. Odutemowo, E.G. Njoroge, T.T. Hlatshwayo, C.C. Theron, Ion bombardment of glassy carbon, Vacuum 149 (2018) 19-22.

19. J.B. Malherbe, O.S. Odutemowo, C.C. Theron, E. Wendler, Diffusion of strontium implanted in glassy carbon, Trans. Royal Soc. A. (2021) Accepted for publication.

20. R.J. Kuhudzai, J.B. Malherbe, T.T. Hlatshwayo, N.G. van der Berg, A. Devaraj, Z. Zhu and M. Nandasiri, Synergistic effects of iodine and silver ions co-implanted in 6H-SiC, J. Nucl. Mater. 467 (2015) 582-587.

21. O.S. Odutemowo, J.B. Malherbe, L. Prinsloo, D.F. Langa and E Wendler, High temperature annealing studies of strontium ion implanted glassy carbon, Nucl. Instrum. Methods Phys. Res. B 371 (2016) 332-335.

22. M. Smoluchowski, Drei Vorträge über Diffusion, Brownsche Molekularbewegung und Koagulation von Kolloidteilchen, Phys. Z. 17 (1916) 557–571: 585–599.

23. J.B. Malherbe, P.A. Selyshchev, O.S. Odutemowo, C.C. Theron, E.G. Njoroge, D.F. Langa, T.T. Hlatshwayo, Diffusion of a mono-energetic implanted species with a Gaussian profile, Nucl. Instrum. Methods Phys. Res. B 406 (2017) 708-713.

24. J.B. Malherbe, Sputtering of compound semiconductor surfaces. II Compositional changes, radiation-induced topography and damage, Crit. Rev. Solid State Mater. Sci. 19 (1994) 128 - 195.

25. E. Friedland, T. Hlatshwayo, N van der Berg, Influence of radiation damage on diffusion of fission products in silicon carbide, Phys Status Solidi C 2 (2013) 208-215.

26. J.B. Malherbe, Sputtering of compound semiconductor surfaces. I. Ion-solid inter-actions and sputtering yields, Crit. Rev. Solid State Mater. Sci. 19 (1994) 55 – 127.

27. E. Friedland, T. Hlatshwayo, N. van der Berg, Influence of radiation damage on diffusion of fission products in silicon carbide, Phys Status Solidi C, 2 (2013), 208-215.

28. J.B. Malherbe, Sputtering of compound semiconductor surfaces. I. Ion-solid inter-actions and sputtering yields, Crit. Rev. Solid State Mater. Sci., 19 (1994), 55-127.

29. W.D. Kingery, H.K. Bowen, D.R. Uhlmann. I. Introduction to Ceramics**,** (2nd ed.), Wiley (1976). Chap. 4.